

Catastrophic onset of fast magnetic reconnection with a guide field

P. A. Cassak^{a)} and J. F. Drake
University of Maryland, College Park, Maryland 20742

M. A. Shay
University of Delaware, Newark, Delaware 19716

(Received 25 January 2007; accepted 4 April 2007; published online 11 May 2007)

It was recently shown that the slow (collisional) Sweet-Parker and the fast (collisionless) Hall magnetic reconnection solutions simultaneously exist for a wide range of resistivities; reconnection is bistable [Cassak, Shay, and Drake, *Phys. Rev. Lett.*, **95**, 235002 (2005)]. When the thickness of the dissipation region becomes smaller than a critical value, the Sweet-Parker solution disappears and fast reconnection ensues, potentially explaining how large amounts of magnetic free energy can accrue without significant release before the onset of fast reconnection. Two-fluid numerical simulations extending the previous results for anti-parallel reconnection (where the critical thickness is the ion skin depth) to component reconnection with a large guide field (where the critical thickness is the thermal ion Larmor radius) are presented. Applications to laboratory experiments of magnetic reconnection and the sawtooth crash are discussed. © 2007 American Institute of Physics. [DOI: 10.1063/1.2734948]

A long-standing puzzle about magnetic reconnection is to explain why systems with magnetic free energy remain outwardly stable for long times with very little magnetic energy release before a sudden onset of reconnection begins the rapid release of the stored energy. This occurs, for example, in solar eruptions and the sawtooth crash in fusion devices.

A great deal of progress has been made in explaining how magnetic energy is rapidly released once onset occurs. While magnetic energy is released very slowly during (collisional) Sweet-Parker reconnection,^{1,2} the energy release during (collisionless) Hall reconnection is as fast as seen in observations.^{3,4} Of particular importance to the present study, simulations and theory⁵⁻⁹ of reconnection with a strong out of plane (guide) magnetic field showed the importance of the Hall and electron pressure gradient terms in achieving fast reconnection. Hall reconnection is fast because the dispersive standing whistler or kinetic Alfvén waves generating reconnection outflow set up the Petschek open outflow (X-type) configuration.^{10,11} Signatures of Hall reconnection have been observed in the Earth's magnetosphere¹²⁻¹⁵ and in laboratory devices.^{16,17}

It is imperative to explain why fast (Hall) reconnection does not always occur. If reconnection is always fast, free magnetic energy cannot accumulate, precluding large explosions. Recently, it was shown that reconnection is bistable; namely, the Sweet-Parker and Hall solutions are both potentially accessible for a wide range of collisionalities.¹⁸ The configuration the system takes is history dependent. Furthermore, the edge of the bistable region is abrupt; the Sweet-Parker and Hall solutions disappear catastrophically beyond critical values of a normalized resistivity, $\eta' = \eta c^2 / 4\pi c_{A,up} d_i$, where η is the classical resistivity, $c_{A,up} = B_{up} / (4\pi m_i n)^{1/2}$ is the ion Alfvén speed based on the density

n and the component of the reconnecting magnetic field B_{up} immediately upstream of the dissipation region, and $d_i = c / \omega_{pi}$ is the ion skin depth, where ω_{pi} is the ion plasma frequency. Coupling to the whistler wave due to the Hall effect begins at the scale length d_i .

As discussed in Ref. 18, this result provides a potential solution to the onset problem. In a system that goes unstable to reconnection, the magnetic field upstream of the dissipation region B_{up} is initially very small. Thus, the normalized resistivity η' is very large and the system undergoes Sweet-Parker reconnection. Since the rate of energy release during Sweet-Parker reconnection is low, magnetic energy can accumulate. As reconnection proceeds, the upstream magnetic field B_{up} increases, which decreases the parameter η' . A transition to Hall reconnection occurs when η' crosses a critical value.¹⁹ This explosively releases the magnetic free energy.

The bistability of reconnection was verified with numerical simulations in Ref. 18 for the special case of anti-parallel reconnection. The Sweet-Parker solution disappears when the thickness of the Sweet-Parker dissipation region $\delta_{SP} = L_{SP}(\eta c^2 / 4\pi c_{A,up} L_{SP})^{1/2}$, where L_{SP} is the length of the Sweet-Parker dissipation region falls below d_i . In the present paper, we extend the result to the more generic case of reconnection with a guide field, which is relevant to fusion plasmas and probably the solar corona.²⁰ We show that the transition from Sweet-Parker to Hall reconnection occurs when δ_{SP} falls below the ion Larmor radius $\rho_s = c_s / \Omega_{ci}$, where $c_s = (T/m_i)^{1/2}$ is the ion sound speed, $\Omega_{ci} = eB/m_i c$ is the ion cyclotron frequency, T is the total temperature, and B is the magnitude of the total magnetic field strength. The length scale ρ_s is introduced by the electron pressure gradient^{6,7,21,22} and is the length scale at which coupling to the kinetic Alfvén wave begins.¹¹

The condition that the Sweet-Parker solution exists, i.e., $\delta_{SP} > \rho_s$, can be written as

^{a)}Present address: Department of Physics and Astronomy, 217 Sharp Laboratory, University of Delaware, Newark, DE 19716

$$\eta' > \eta'_{\text{sf}}, \quad (1)$$

where $\eta' = \eta c^2 / 4\pi c_{A,\text{up}} d_i$ is the normalized resistivity, defined in this way to be consistent with the anti-parallel definition, and $\eta'_{\text{sf}} = \rho_s^2 / d_i L_{\text{SP}}$. If a system is undergoing Sweet-Parker reconnection and η' decreases, Sweet-Parker reconnection will continue provided $\eta' > \eta'_{\text{sf}}$.

Just as in the anti-parallel case, the condition that the Hall solution exists is that diffusion $\eta c^2 / 4\pi \delta_e^2$ of magnetic fields in the electron dissipation region is dominated by convection $v_{\text{in},e} / \delta_e$ of magnetic fields into the electron dissipation region, where $v_{\text{in},e}$ is the electron inflow speed into the electron dissipation region of thickness δ_e . How do δ_e and $v_{\text{in},e}$ scale in component reconnection? Particle simulations have revealed that δ_e scales like the electron Larmor radius.^{23,24} In the fluid simulations to follow, nongyrotropic elements of the electron pressure tensor are not retained, so the electron frozen-in condition is broken by electron inertia and δ_e scales like the electron skin depth $d_e = c / \omega_{\text{pe}}$, where ω_{pe} is the electron plasma frequency. The scaling of the inflow speed with system parameters has not been fully explored. In anti-parallel reconnection, the inflow speed scales like $v_{\text{in},e} \sim 0.1 c_{A,e,\text{up}}$,^{3,25} where $c_{A,e,\text{up}}$ is the electron Alfvén speed based on the magnetic field $B_{e,\text{up}}$ immediately upstream of the electron dissipation region. This speed is also the phase speed of the whistler wave evaluated with $k \sim 1/d_e$. By analogy, one might expect the outflow speed for component reconnection to be the phase speed of the kinetic Alfvén wave evaluated with $k \sim 1/\delta_e \sim 1/d_e$, which is $v_{\text{ph}} \sim \beta^{1/2} c_{A,e,\text{up}}$, where $\beta = c_s^2 / c_A^2$ is the plasma β . While this result has not been established numerically, results of a benchmark simulation were consistent with this scaling. Taking the inflow speed $v_{\text{in},e}$ to scale like $0.1 v_{\text{ph}}$, the Hall reconnection validity condition can be written as

$$\eta' < \eta'_{\text{fs}}, \quad (2)$$

where $\eta'_{\text{fs}} \sim 0.1 \beta^{1/2} B_{e,\text{up}} / B_{\text{up}}$. If a system is undergoing Hall reconnection and η' increases, Hall reconnection will continue as long as $\eta' < \eta'_{\text{fs}}$.

The range in η' for which reconnection is bistable is, therefore, $\eta'_{\text{sf}} < \eta' < \eta'_{\text{fs}}$. The ratio of the critical η' scales is $\eta'_{\text{sf}} / \eta'_{\text{fs}} \sim 10 B_{\text{up}} \rho_s / B_{e,\text{up}} L_{\text{SP}}$, which is small because $\rho_s \ll L_{\text{SP}}$ for systems of physical interest. Thus, bistability is present over a wide range η' , just as in the anti-parallel case.

To numerically demonstrate bistability of reconnection for $\eta'_{\text{sf}} < \eta' < \eta'_{\text{fs}}$, we use the same technique as in Ref. 18. Namely, we show that a system undergoing Hall reconnection with a resistivity below η'_{fs} continues to do so for any value of resistivity below this value. We then show that a system undergoing Sweet-Parker reconnection with a resistivity above η'_{sf} will continue to do so for any value of resistivity above this value.

The simulations are performed using the massively parallel two-fluid code F3D²⁶ in a periodic two-dimensional domain with a slab geometry of size $L_x \times L_y = 204.8 d_i \times 102.4 d_i$ and a cell size of $0.05 d_i \times 0.05 d_i$. The initial equilibrium is two Harris sheets in a double tearing mode configuration; i.e., $\mathbf{B} = \hat{\mathbf{x}} B_0 (\tanh[(y + L_y/4)/w_0] - \tanh[(y - L_y/4)/w_0] - 1) + \hat{\mathbf{z}} B_g$ with $B_g = 5 B_0$ and $w_0 = 1 d_i$. The ions

are initially stationary and initial pressure balance is enforced by a nonuniform density. The plasma is isothermal for simplicity. A coherent perturbation of amplitude $0.002 B_0$ is seeded over the equilibrium magnetic field to induce reconnection. The resistivity η is uniform. A small fourth-order dissipation, i.e., $\propto \eta_4 \nabla^4$ with $\eta_4 = 2 \times 10^{-5}$, is used in all of the equations to discourage secondary island formation. Lengths are normalized to $d_i = (m_i c^2 / 4\pi n_0 e^2)^{1/2}$, velocities to $c_{A0} = B_0 / (4\pi m_i n_0)^{1/2}$, resistivities to $\eta_0 = 4\pi c_{A0} d_i / c^2$, and electric fields to $E_0 = B_0 c_{A0} / c$, where n_0 is the density far from the current sheets.

The temperature is fixed at $T_0 = 5 B_0^2 / 4\pi m_0$, making the total plasma $\beta = 4\pi n T / B^2 \approx 0.19$ far from the sheet and the in-plane $\beta_{\text{rec}} = 4\pi n T / B_0^2 = 5$. These values were chosen to be in the kinetic Alfvén wave regime with $\beta_{\text{rec}} \gg 1 \gg \beta$.¹¹ The electron mass is $m_e = m_i / 25$ (i.e., $d_e = c / \omega_{\text{pe}} = 0.2 d_i$). Although this value is unrealistic, the electron mass only controls dissipation at the electron scales, which does not greatly impact the rate of component Hall reconnection,^{27,28} so the results should be insensitive to m_e .

For this computational domain, we estimate the predictions for η'_{sf} and η'_{fs} . Since the half-length of the Sweet-Parker layer L_{SP} scales with the system size,²⁹⁻³¹ $L_{\text{SP}} \sim L_x / 4 \approx 50 d_i$. Benchmark resistive-MHD simulations put the value closer to $L_{\text{SP}} \approx 38 d_i$. Using $\rho_s^2 = \beta d_i^2$, one finds

$$\eta'_{\text{sf}} = \frac{\rho_s^2}{d_i L_{\text{SP}}} = \frac{\beta d_i}{L_{\text{SP}}} \approx 0.005, \quad (3)$$

From benchmark simulations of Hall reconnection, the magnetic field strength upstream of the electron and ion dissipation regions are $B_{e,\text{up}} \approx 0.35 B_0$ and $B_{\text{up}} \approx 0.8 B_0$, so

$$\eta'_{\text{fs}} \sim 0.1 \beta^{1/2} \frac{B_{e,\text{up}}}{B_{\text{up}}} \approx 0.019. \quad (4)$$

We emphasize that these scales differ by only a factor of 4 because of computational constraints; a larger domain would lead to a more realistic separation in scales because $\eta'_{\text{sf}} / \eta'_{\text{fs}} \propto L_{\text{SP}}^{-1} \propto L_x^{-1}$, but would be computationally prohibitive.

A benchmark collisionless ($\eta=0$) Hall-MHD simulation is evolved from $t=0$ until a steady-state of Hall reconnection is reached, with a reconnection rate of $E \approx 0.065 E_0$. This is plotted as a function of island width w as the thick solid line in Fig. 1. Since the island width increases monotonically in time, w is a proxy for the time t . The reconnection rate is calculated as the time rate of change of magnetic flux between the X-line and O-line. When $w \approx 17 d_i$, a resistivity of $\eta = 0.010 \eta_0$ (which lies between the predicted values of η'_{sf} and η'_{fs}) is enabled and the simulation is continued until most of the available magnetic flux has reconnected. For comparison, the thick dashed line shows the reconnection rate when $\eta=0$ is maintained. A slight decrease in the reconnection rate is observed, but the system clearly remains in the Hall solution, with the characteristic Petschek open outflow configuration of component Hall reconnection.^{5,7,23,27,28,32-38}

Similarly, a benchmark resistive-MHD simulation with $\eta = 0.010 \eta_0$ (the same resistivity), with the Hall and electron inertia terms disabled, is performed. As shown in the thin solid line of Fig. 1, the reconnection rate reaches a steady

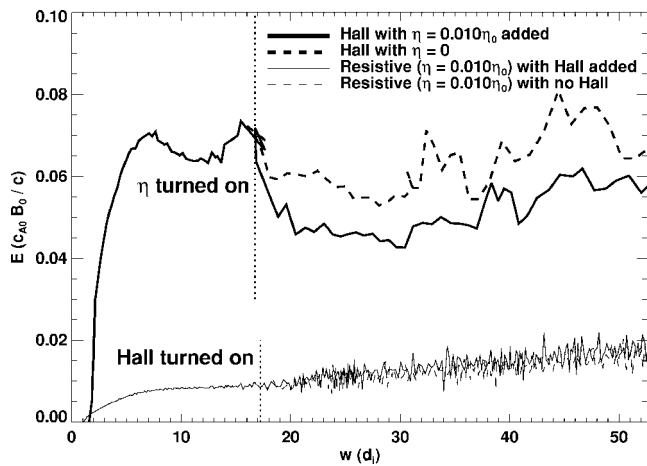


FIG. 1. Reconnection rate E as a function of island width w for the two sets of simulations described in the text. The vertical dotted lines show when the added effects were enabled. Note that the final parameters of the two solid line simulations are identical.

value at about $E \approx 0.01E_0$. When $w \approx 17d_i$, we enable the Hall and electron inertia terms and continue to advance the full equations. The reconnection rate remains stationary with $E \approx 0.01E_0$. For comparison, a simulation in which the Hall term is not enabled is shown as the thin dashed line in Fig. 1. Clearly, the Hall and electron inertia terms do not impact the rate of reconnection for these parameters; the system remains in the Sweet-Parker solution with the characteristic elongated current sheet of Sweet-Parker reconnection.^{1,2,29–31} The two configurations are governed by the same equations and have the same resistivity, so the bistability of component reconnection for this value of the resistivity is demonstrated.

The range in η of the bistable regime is found by varying the resistivities of the benchmark Hall and Sweet-Parker reconnection simulations of Fig. 1. For the case of Hall reconnection, we change η from 0.0 to 0.005, 0.007, 0.010, 0.0125, 0.015, 0.0175, and $0.020\eta_0$ when $w \approx 17d_i$. For the case of Sweet-Parker reconnection, we change η from $0.010\eta_0$ to 0.003, 0.005, 0.007, 0.0085, 0.0125, 0.015, 0.0175, and $0.020\eta_0$ when $w \sim 20.5d_i$, a short time after the Hall and electron inertia terms have been enabled.

The asymptotic normalized reconnection rate E' , computed as the time averaged reconnection rate once transients have died away and normalized to $B_{\text{up}}c_{A,\text{up}}/c$, is plotted in Fig. 2(a). The simulations starting in Hall reconnection are the open circles, while the closed circles start in Sweet-Parker. The dashed line shows the prediction of the Sweet-Parker model based on benchmark numerical simulation values of $L_{\text{SP}} \approx 38d_i$ and $B_{\text{up}} \approx 0.8B_0$, showing excellent agreement with the Sweet-Parker results. The figure shows that component magnetic reconnection is bistable over a range of resistivities. [The apparent dependence of E' on η during Hall reconnection seen in Fig. 2(a) is unexpected and does not occur in anti-parallel reconnection.¹⁸ It is probably a numerical effect due to the fact that the ion and electron dissipation regions are not well separated in our simulations, as ρ_s is only twice as big as d_e .]

The edge of the bistable region is observed to be abrupt with critical values of η_{sf} between $0.005\eta_0$ and $0.0075\eta_0$,

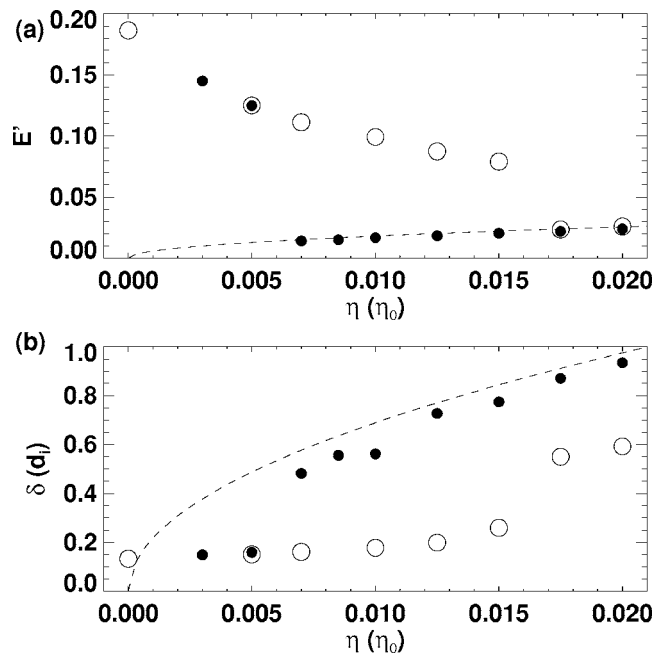


FIG. 2. (a) Normalized steady-state reconnection rate E' as a function of resistivity η for simulations analogous to those in Fig. 1 as described in the text. (b) Current sheet thickness δ as a function of η for the simulations in (a).

and η_{fs} between $0.015\eta_0$ and $0.0175\eta_0$. Normalizing η to η' using $B_{\text{up}} \approx 0.8B_0$ gives simulation values of η'_{sf} between 0.006 and 0.009, and η'_{fs} between 0.019 and 0.022, in good agreement with the scaling law predictions of Eqs. (3) and (4).

The asymptotic steady-state current sheet thickness δ , measured as the half-width at half-maximum of the out-of-plane current density J_z at the X-line, is plotted in Fig. 2(b) for each of the simulations, with the Sweet-Parker prediction plotted as the dashed line. The transition from Sweet-Parker to Hall reconnection (shown in the closed circles) occurs when the thickness of the current sheet is approximately $\rho_s \approx 0.44d_i$, as predicted.

The present result is consistent with recent experimental results at the Versatile Toroidal Facility.³⁹ Bursts of fast reconnection occur in about 10% of experimental trials. Preliminary diagnostics suggest that the thickness of the current sheet at onset is very close to the ion Larmor radius $\rho_s \sim 10$ cm.³⁹

Can the present results explain the onset of the sawtooth crash in fusion devices? The simple model presented here does not include diamagnetic effects, which are important for tokamak plasmas and have been shown to inhibit reconnection.^{40–42} Using parameters at the DIII-D tokamak,⁴³ we find η_{sf} to be too small to explain the observations. The inclusion of diamagnetic effects would make the Sweet-Parker dissipation region wider for a given resistivity, so the agreement should improve. This will be the subject of future studies.

Potential limitations of this model are that the simulations are limited to two dimensions and the resistivity is not evolved with time self-consistently.

ACKNOWLEDGMENTS

This work has been supported by NSF Grant No. PHY-0316197 and DOE Grant Nos. ER54197 and ER54784. Computations were carried out at the National Energy Research Scientific Computing Center.

- ¹P. A. Sweet, in *Electromagnetic Phenomena in Cosmical Physics*, edited by B. Lehnert (Cambridge University Press, New York, 1958), p. 123.
- ²E. N. Parker, *J. Geophys. Res.* **62**, 509 (1957).
- ³M. A. Shay, J. F. Drake, B. N. Rogers, and R. E. Denton, *Geophys. Res. Lett.* **26**, 2163 (1999).
- ⁴J. Birn, J. F. Drake, M. A. Shay *et al.*, *J. Geophys. Res.* **106**, 3715 (2001).
- ⁵A. Y. Aydemir, *Phys. Fluids B* **4**, 3469 (1992).
- ⁶X. Wang and A. Bhattacharjee, *Phys. Rev. Lett.* **70**, 1627 (1993).
- ⁷R. Kleva, J. Drake, and F. Waelbroeck, *Phys. Plasmas* **2**, 23 (1995).
- ⁸L. Zakharov, B. Rogers, and S. Migliuolo, *Phys. Fluids B* **5**, 2498 (1993).
- ⁹X. Wang and A. Bhattacharjee, *Phys. Plasmas* **2**, 171 (1995).
- ¹⁰M. E. Mandt, R. E. Denton, and J. F. Drake, *Geophys. Res. Lett.* **21**, 73 (1994).
- ¹¹B. N. Rogers, R. E. Denton, J. F. Drake, and M. A. Shay, *Phys. Rev. Lett.* **87**, 195004 (2001).
- ¹²X. H. Deng and H. Matsumoto, *Nature* **410**, 557 (2001).
- ¹³M. Øieroset, T. D. Phan, M. Fujimoto, R. P. Lin, and R. P. Lepping, *Nature* **412**, 417 (2001).
- ¹⁴T. Nagai, F. S. Mozer, N. C. Maynard, P. A. Puhl-quinn, Z. W. Ma, and C. T. Russell, *J. Geophys. Res.* **106**, 25,929 (2001).
- ¹⁵F. Mozer, S. D. Bale, and T. D. Phan, *Phys. Rev. Lett.* **89**, 015002 (2002).
- ¹⁶Y. Ren, M. Yamada, S. Gerhardt, H. Ji, R. Kulsrud, and A. Kuritsyn, *Phys. Rev. Lett.* **95**, 055003 (2005).
- ¹⁷C. D. Cothran, M. Landreman, M. R. Brown, and W. H. Matthaeus, *Geophys. Res. Lett.* **32**, L03105, (2005).
- ¹⁸P. A. Cassak, M. A. Shay, and J. F. Drake, *Phys. Rev. Lett.* **95**, 235002 (2005).
- ¹⁹P. A. Cassak, J. F. Drake, and M. A. Shay, *Astrophys. J.* **644**, L145 (2006).
- ²⁰M. Swisdak, J. F. Drake, M. A. Shay, and J. G. McIlhargey, *J. Geophys. Res.* **110**, A05210 (2005).
- ²¹V. M. Vasyliunas, *Rev. Geophys. Space Phys.* **13**, 303 (1975).
- ²²J. F. Drake and Y. C. Lee, *Phys. Fluids* **20**, 1341 (1977).
- ²³M. Hesse, M. Kuznetsova, and M. Hoshino, *Geophys. Res. Lett.* **29**, 1563 (2002).
- ²⁴M. Hesse and J. Birn, *Ann. Geophys.* **22**, 603 (2004).
- ²⁵J. D. Huba and L. I. Rudakov, *Phys. Rev. Lett.* **93**, 175003 (2004).
- ²⁶M. A. Shay, J. F. Drake, M. Swisdak, and B. N. Rogers, *Phys. Plasmas* **11**, 2199 (2004).
- ²⁷P. L. Pritchett, *J. Geophys. Res.* **106**, 3783 (2001).
- ²⁸P. Ricci, J. U. Brackbill, W. Daughton, and G. Lapenta, *Phys. Plasmas* **11**, 4102 (2004).
- ²⁹D. Biskamp, *Phys. Fluids* **29**, 1520 (1986).
- ³⁰D. A. Uzdensky and R. M. Kulsrud, *Phys. Plasmas* **7**, 4018 (2000).
- ³¹B. D. Jemella, J. F. Drake, and M. A. Shay, *Phys. Plasmas* **11**, 5668 (2004).
- ³²M. Tanaka, *Phys. Plasmas* **3**, 4010 (1996).
- ³³R. Horiuchi and T. Sato, *Phys. Plasmas* **4**, 277 (1997).
- ³⁴E. Cafaro, D. Grasso, F. Pegorano, F. Porcelli, and A. Saluzzi, *Phys. Rev. Lett.* **80**, 4430 (1998).
- ³⁵M. Hesse, K. Schindler, J. Birn, and M. Kuznetsova, *Phys. Plasmas* **6**, 1781 (1999).
- ³⁶B. N. Rogers and R. E. Denton, *J. Geophys. Res.* **108**, 1111, (2003).
- ³⁷P. L. Pritchett and F. V. Coroniti, *J. Geophys. Res.* **109**, 1220, (2004).
- ³⁸J. D. Huba, *Phys. Plasmas* **12**, 012322 (2005).
- ³⁹J. Egedal, W. Fox, N. Katz, M. Porkolab, K. Reim, and E. Zhang, *Phys. Rev. Lett.* **98**, 015003 (2007).
- ⁴⁰B. Rogers and L. Zakharov, *Phys. Plasmas* **2**, 3420 (1995).
- ⁴¹M. Swisdak, J. F. Drake, M. A. Shay, and B. N. Rogers, *J. Geophys. Res.* **108**, 1218 (2003).
- ⁴²K. Germaschewski, A. Bhattacharjee, C. S. Ng, X. Wang, and L. Chacon, *Bull. Am. Phys. Soc.* **51**, 312 (2006).
- ⁴³E. A. Lazarus, F. L. Waelbroeck, T. C. Luce *et al.*, *Plasma Phys. Controlled Fusion* **48**, L65 (2006).